Techno-economic-environmental analysis of seasonal thermal energy storage with solar heating for residential heating in China

Tianrun Yang [a], Wen Liu [a,*], Qie Sun [b], Weihao Hu [c], Gert Jan Kramer [a]

[a] Copernicus Institute of Sustainable Development, Utrecht University, Princetonlaan 8a, 3584 CB, Utrecht, the Netherlands
[b] Institute of Thermal Science and Technology, Shandong University, Jingshi Road 17923, Jinan, 250061, China
[c] School of Mechanical and Electrical Engineering, University of Electronic Science and Technology of China, Chengdu, 611731, China

ARTICLE INFO

ABSTRACT

Seasonal thermal energy storage (STES) of solar heat is an option of interest for clean heat transition, as residential heating is often fossil fuel-based. This study 1) proposes an integrated optimization criterion to examine how local context influences the optimal configuration planning, techno-economic-environmental performance, and feasibility of STES application; 2) identifies the position of STES in comparison to other sustainable heating options considering the local context; and 3) provides a comprehensive and transparent showcase highlighting the importance of the local context in determining the feasibility of STES in the clean heating transition. The TRNSYS modeling tool is adopted to analyze the performance, and Pareto optimization is applied to treat the multi-objective optimization. The solar fractions and storage efficiencies of the four case studies range between 58-67% and 57–69%, respectively. STES has significant potential to reduce CO_2 emissions (52–72%) compared to conventional heating systems. However, the heating cost of the STES system (5.4–8.7 €-ct/kWh) is more than twice that of the conventional heating system. The CO_2 avoidance cost of the four case studies ranges between 114 and 368 €/t. Properly reducing the borehole number in cold climate zones and increasing the solar collector area in warm climate zones help improve the system performance.

1. Introduction

Energy storage is essential in transitioning from a fossil fuel-to a renewable energy-based energy system, especially in the context of future smart energy systems, since most renewable energy sources are discontinuous [1]. Compared with electricity storage, heat storage provides an option for system balancing and flexibility with lower costs [2]. Heat storage in smart energy systems can facilitate the utilization of multiple renewable energy sources, integrate waste heat and cool, and balance the electrical network [3]. The 5th generation district heating (DH) also highlights the importance of heat storage [4].

Due to the seasonal variations of heating, long-term thermal energy storage in the form of seasonal thermal energy storage (STES) is preferable to coordinate the seasonal mismatch between heat supply and demand. Depending on their storage mechanisms, STES can be classified into three main types: sensible heat storage, latent heat storage, and thermochemical heat storage, of which sensible heat storage (using a water tank, pit, borehole, and aquifer) is mature and mass-market. The main heat sources include solar thermal energy, industrial waste heat,

and geothermal energy. Heat pumps, gas boilers, and electrical heaters are widely used as auxiliary heating devices in case STES fails to meet the heat demand [5].

After decades of development, multiple technologies for STES have been implemented [6,7]. The development of STES has been extensively studied and reviewed from a technical perspective [8,9]. Xu et al. [10] introduced the technical performance of a demonstrated 2304 m^2 solar-heated greenhouse with 4970 m^3 soil to store the heat collected by 500 m^2 solar collectors. Guo et al. [6] proposed a large-scale STES integrated with an industrial waste heat heating system and an absorption heat pump and assessed its long-term performance. Kim et al. [11] introduced an STES system for a community comprising 300 energy-plus residential houses in South Korea. The results showed that the STES system reduced by 17% CO_2 emissions with a 6-year payback period compared to the gas boiler system. Salvestroni et al. [12] designed an STES with a 3800 m^3 hot water tank and 1000 m^2 solar collectors, achieving a solar fraction (SF) of 40%.

The previous review analysis has concluded that STES economic studies are limited in number and often lack transparency in their reporting [5]. Several STES implementations were reviewed, as listed in

Nomenclature

E	energy
G	incident solar irradiance
I	investment cost
m	mass
n	lifetime
Q	thermal energy
r	discount rate
T	temperature
t	time

Greek symbols

ΔCO_2	CO_2 emission saving
η	efficiency
μ	CO_2 equivalent emission factor

Abbreviations

ATES	aquifer thermal energy storage
BB	biomass boiler
BTES	borehole thermal energy storage
CCS	carbon capture and storage
CHP	combined heat and power
COP	coefficient of performance
DH	district heating
DHW	domestic hot water
DLSC	Drake Landing Solar Community
GH	geothermal heating
GHI	global horizontal irradiance

GSHP	ground source heat pump
HDD	heating degree day
LCOE	levelized cost of energy
LCOH	levelized cost of heat
NGB	natural gas boiler
O&M	operation and maintenance
PTES	pit thermal energy storage
SF	solar fraction
STES	seasonal thermal energy storage
TRT	thermal response test
TTES	tank thermal energy storage

Superscripts

boreh	borehole
cs	conventional system

Subscripts

amb	ambient
arr	solar collector array
charg	charge
disch	discharge
el	electricity
in	inlet
s	storage
setp	setpoint
sol	solar
th	thermal
tot	total

Table 1. Those studies have concluded that STES positively impacts the clean heat transition. The technical performance of STES projects has been examined through experiments and simulations. However, there is a lack of in-depth insights into economic and environmental performances to provide the facts on the position of STES applications compared with other sustainable heating technologies. There is a need for a comprehensive quantitative method for the techno-economic-environmental performance analysis of STES applications.

The existing studies focus primarily on technical performance assessment and analysis instead of optimization. Within the optimization research, Huang et al. [15] aimed to optimize the system based on

Table 1
Review of STES applications.

Study	Country	Heated area	Main heat source	Inclusion of technical/ economic/environmental analysis	Economic and environmental indicator	Inclusion of performance analysis/parametric study/ optimization	Objective function of optimization
[13]	China	400,000 m^2	Waste heat + solar energy	+/−/−		+/+/−	
[14]	Canada	A greenhouse	Solar energy	+/+/−	Levelized cost of energy (LCOE)	+/−/−	
[15]	China	19,000 m^2	Solar energy	+/+/−	Investment	+/+/+	Renovation cost
[16]	Sweden	A factory	Waste heat	+/−/−		+/−/−	
[17]	China	A university campus	Solar energy	+/−/−		+/−/−	
[18]	Italy	Six houses	Solar energy	+/+/+	Investment, CO_2 emission saving	+/+/−	
[19]	China	A university campus	Solar energy	+/−/−		+/−/−	
[20]	France	Eight houses	Solar energy	+/+/−	LCOE	+/+/+	SF, solar collector efficiency, LCOE
	China	2,304 m^2	Solar energy	+/−/−		+/−/−	
[12]	Italy	20,207 m^2	Solar energy	+/−/−		+/+/−	
[21]	China	500 m^2	Solar energy	+/−/−		+/−/−	
[22]	Switzerland	35 buildings	Solar energy	+/+/+	yearly cost, CO_2 emissions	+/−/+	Yearly cost
[23]	China	–	Waste heat	+/−/−		+/+/−	
[24]	Denmark	–	Solar energy	+/−/−		+/−/−	
[25]	China	1,500 m^2	Solar energy	+/−/−		+/−/−	
[26]	Finland	31,100 m^2	Solar energy	+/+/+	Life cycle cost, LCOE, CO_2 emissions	+/−/+	Heat production, LCOE

($+ \triangleq$ included; $- \triangleq$ not included).

minimum renovation cost by testing different water tank sizes. However, the method was a parametric study rather than an optimization. Launay et al. [20] proposed a strategy for multi-criteria optimization using SF, solar collector efficiency, and LCOE as objectives. Fiorentini's optimization aimed to minimize the yearly cost of the energy system [22]. Indicators of environmental performance were missing in these studies. Yuan et al. [26] aimed to find out the optimal solution with high performance and low costs. Shah et al. [27] used minimum life cycle cost and greenhouse gas emissions as objective functions and total solar collector area and borehole length as optimizing variables to optimize the STES systems in six selected cold climate locations. They obtained several optimal solutions for each specific site without a generic conclusion. It failed to identify the key parameters and quantify their influence on the optimization results. There is a need for a better understanding of the optimal economic and environmental performance of STES applications and the conditions to achieve it. It requires an integrated optimization criterion and method to select the optimal solution.

The hypothesis of this study is that the local context plays an important role in the optimal configuration planning, techno-economic-environmental performance, and feasibility of the STES application. The techno-economic-environmental performance and feasibility of STES in cold climates are preferable to those in warm climates. The key influential parameters in determining the optimal performance differ based on climate conditions. With the knowledge gaps discussed above, the main contributions of this study are summarized as two aspects. From the methodological perspective, previous studies on the optimization of STES failed to identify the key parameters and quantify their influence on the optimization results. There is a need for a better understanding of the optimal economic and environmental performance of STES applications and the conditions to achieve it. Therefore, an integrated optimization criterion (CO_2 avoidance cost) is proposed to select the optimal solution and determine the optimization pathways for different climates. By applying this indicator in the optimization, three research questions are answered: 1) How do the local climate condition and existing heating infrastructure influence the CO_2 avoidance cost of STES? 2) What are the key technical parameters in achieving the optimal techno-economic-environmental performance of STES in different climate zones? 3) What is the position of STES in comparison to other sustainable heating options in terms of CO_2 avoidance cost considering the local context? From the case study perspective, China accounts for 40% of global DH production, with a 30% higher CO_2 emissions intensity than the world average [28]. This study presents four local-specific cases at a community level in representative climate conditions that consider local circumstances and makes an effort to provide an informative and transparent presentation based on regional specificity. It provides a comprehensive and transparent showcase highlighting the importance of context in determining the feasibility of STES in the clean heating transition at the local level.

2. Methodology

In this study, a four-step methodology was proposed and applied to fulfill the research objective, as shown in Fig. 1. In this analysis, the technical, economic, and environmental performance of implementing an STES system was investigated in four locations in China: Harbin, Urumqi, Shanghai, and Chengdu. Moreover, a parametric study was conducted to investigate how the system configurations influence the overall performance. Furthermore, multi-objective optimization was performed with the minimum levelized cost of heat (LCOH) and CO_2 emissions as the objective functions. Based on the optimization, the CO_2 avoidance cost was obtained, and optimal solutions were selected with the minimum CO_2 avoidance cost criteria.

2.1. TRNSYS model development

Research and demonstration of STES applications in China have
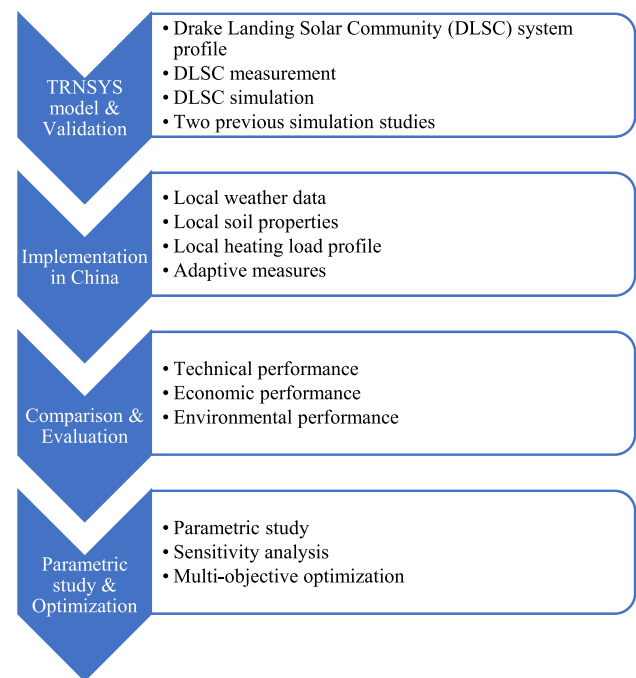

Fig. 1. Schematic of the methodology employed in this study.

mainly included tank thermal energy storage (TTES) and borehole thermal energy storage (BTES) [29]. The low storage density and high cost of TTES are unsuitable for the high population density of China [5]. Also, the BTES system can substantially improve the system performance in terms of mismatch reliving and CO_2 emission reduction, while tank storage has fewer benefits [30]. Therefore, the BTES was chosen for the analysis in this study. Several pilot BTES projects exist in China; however, their data remain unpublicized.

In this study, a BTES system was modeled using the TRNSYS [31] simulation tool, based on the DLSC system schematic design located in Okotoks, Canada (presented in Fig. 2). The project was well regarded as a successful STES application, and the data are transparent [32,33]. The system comprises 2293 m^2 flat-plate glazed collectors, two 120 m^3 short-term storage tanks, and 144 boreholes with a diameter of 35 m and a depth of 37 m. The system supplies the space and water heating for 52 houses with a total heated living area of 7540 m^2. The DLSC system was commissioned in 2007, achieving consistent SFs above 90% since the fifth year of operation. More information about the DLSC system can be found in Refs. [34,35]. The simulation covered five years, from July 1, 2007, to June 30, 2012. The time step was set as 10 min since the measurements of the DLSC were on a 10-min basis [36]. An illustration of the TRNSYS model and detailed input data, including weather data, solar collector loop, short-term storage loop, borehole loop, and load loop, is presented in Supplementary materials.

2.2. Validation

It is necessary to validate the model before implementing it in China. Accordingly, the DLSC measurements, DLSC simulation results, and two previous simulation results of the DLSC system from peer-reviewed articles were used to validate the model developed in this study.

2.3. Comparison and evaluation

Implementation was evaluated through several performance indicators from technical, economic, and environmental perspectives.
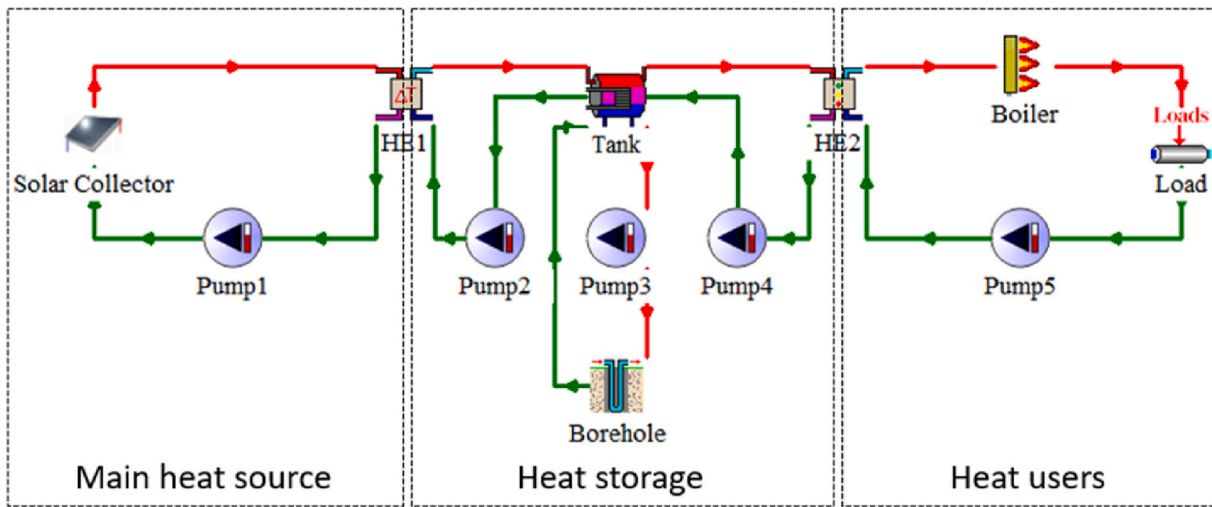
Fig. 2. Simplified diagram of the STES model system.

2.3.1. Technical performance

Generally, the technical performance of an STES system is described by its SF and storage efficiency. The SF indicates the percentage of the heating load that can be met by solar thermal energy; it can be expressed as follows:

$$SF = \frac{E_{th,sol}}{E_{th,tot}} = \frac{E_{th,sol}}{E_{th,sol} + E_{th,boil}} \tag{1}$$

where $E_{th,sol}$ denotes the heating load met by solar thermal energy, $E_{th,tot}$ represents the total thermal energy supplied to the users, and $E_{th,boil}$ corresponds to the thermal energy provided by the auxiliary natural gas boiler (NGB).

The performance of the borehole was evaluated based on the storage efficiency, illustrating the efficiency of the borehole:

$$\eta_s = \frac{E_{th,disch}^{boreh}}{E_{th,charg}^{boreh}} \tag{2}$$

where $E_{th,disch}^{boreh}$ denotes the thermal energy discharged from the borehole, and $E_{th,charg}^{boreh}$ corresponds to the thermal energy charged into the borehole.

2.3.2. Economic performance

Economic performance was assessed by calculating the LCOH for the following purposes. First, the relative economic competitiveness of implementing the STES scheme in different climate zones was evaluated. Accordingly, the LCOHs of the STES applications at the four locations were compared. Second, the LCOH of the STES application was compared with the cost of existing heat supply technology to position the STES project in the local heat market. Lastly, an LCOH comparison of the STES system in China, the DLSC system, and the benchmark case in Europe was performed. The LCOH was determined as follows:

$$LCOH = \frac{I + \sum_{t=1}^{n} \frac{O\&M}{(1+r)^t}}{\sum_{t=1}^{n} \frac{E_{th}}{(1+r)^t}} \tag{3}$$

where I denotes the initial investment, r represents the discount rate, n is the lifetime, $O\&M$ symbolizes the annual operation and maintenance cost, and E_{th} corresponds to the annual heat production.

The heating costs of the conventional systems were calculated as [37]:

$$Heating\ cost = \frac{Depreciation + O\&M}{Heat\ production} \tag{4}$$

An illustration of the investment costs, annual operation and maintenance costs, electricity and natural gas prices, lifetime, and discount rate is presented in Supplementary materials.

2.3.3. Environmental performance

The environmental performance of the STES system was evaluated by CO_2 emission savings. The mass of CO_2 emitted while consuming energy was calculated as

$$m_{CO_2} = \mu_{CO_2}^E \bullet E \tag{5}$$

where $\mu_{CO_2}^E$ denotes the CO_2 equivalent emission factor, and E represents the energy consumption.

The CO_2 emission saving was determined by comparing the CO_2 emissions of the conventional system with that of the proposed STES system:

$$\Delta CO_2 = m_{CO_2}^{cs} - m_{CO_2}^{STES} \tag{6}$$

where $m_{CO_2}^{CS}$ and $m_{CO_2}^{STES}$ represent the CO_2 emissions of the conventional system and the STES system, respectively, which can be calculated as

$$m_{CO_2}^{cs} = \mu_{CO_2}^{th} \bullet E_{th} \tag{7}$$

$$m_{CO_2}^{STES} = \mu_{CO_2}^{el} \bullet E_{el} + \mu_{CO_2}^{th} \bullet E_{th} \tag{8}$$

where $\mu_{CO_2}^{th}$ and $\mu_{CO_2}^{el}$ respectively, denote the CO_2 equivalent emission factors of heating and electricity production, and E_{th} and E_{el} indicate the heating and electricity consumption, respectively. The CO_2 equivalent emission factors used for the four locations are presented in Supplementary materials.

2.4. Parametric study and optimization

A parametric study was conducted to investigate the impact of system configurations on the technical, economic, and environmental performance of the STES system and provide evidence for optimization. The tested system configurations included the solar collector area, short-term storage tank volume, and the borehole number. The indicators used in the parametric study included SF, LCOH, and CO_2 emission savings. Besides, a sensitivity analysis was conducted to investigate the influence of the equipment unit prices, discount rate, and electricity and natural gas prices on the LCOH calculation.

The minimum LCOH and the minimum CO_2 emissions of the STES system were chosen as the multi-objective functions for optimization, with economic feasibility and environmental impact considered as two

crucial factors. The solar collector area and borehole number were selected as the main variables in the optimization. The optimal solutions for the STES system were obtained through Pareto optimization. One Pareto front was obtained for each case by changing relevant parameters, running simulations, and calculating LCOH and CO_2 emissions. Moreover, the CO_2 avoidance cost was determined based on the Pareto front, which describes the cost of CO_2 emission reduction of the proposed system compared with the conventional system, providing a useful way of comparing the costs of various methods of reducing emissions. The optimal solution was selected from the Pareto front by minimum CO_2 avoidance cost criteria. CO_2 avoidance cost can be calculated as follows:

$$CO_2\ avoidance\ cost = \frac{Heating\ cost\ of\ STES\ system - Heating\ cost\ of\ conventional\ system}{CO_2\ emission\ saving} \qquad (9)$$

3. Case study

In China, 80% of the demand for heating of urban buildings in northern areas is supplied by DH systems [38]. The total heated area increased by 112%, and the total heat supply amount increased by 35% from 2010 to 2019 [39]. The Chinese government issued the *Winter clean heating plan (2017–2021) for northern China* in 2017 and the 14th *five-year plan and vision 2035* in 2021. These planning policies aim to support renewable energy heating and promote a clean heat transition in northern areas, where STES systems may play a role in facilitating the decarbonization of heat supply systems. In southern China, it has been reported that promoting DH in suitable areas can improve residential welfare and potentially bring economic and environmental benefits [40].

Generally, solar radiation is abundant in China; over two-thirds of the territory receives an irradiance of more than 5000 MJ/m² and more than 2200 h of sunshine annually [41]. Fig. 3 illustrates the solar resources distribution. Regarding solar heat applications, 70% of the global solar collector installations are in China [42], which further highlights the potential of STES applications in DH in China.
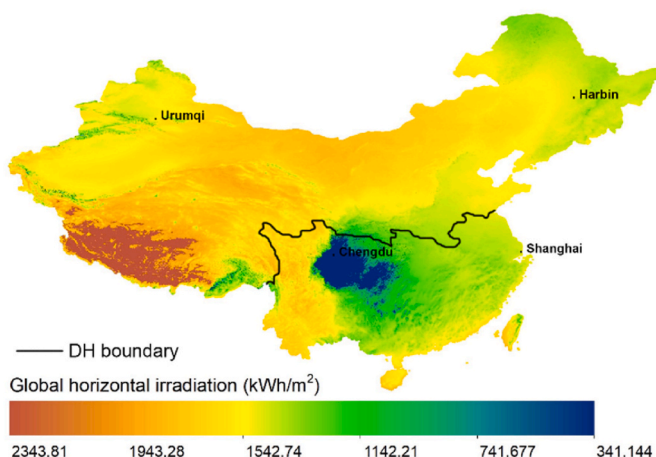

Fig. 3. Solar resources in China [43].

3.1. Local properties

The DH and non-DH areas in China were set according to the "Qin Mountains-Huai River" boundary, named the north-south heating line [40]. As shown in Fig. 3, Harbin and Urumqi are located in northern China with a DH system, while Shanghai and Chengdu do not have a DH system in southern China. The climatic conditions of the four locations are listed in Table 2. The four locations have different heating loads and solar resources. Fig. 4 illustrates the monthly average temperature and average global horizontal irradiance (GHI) at the four locations.

3.2. Implementation in China

The validated model was implemented in four locations in China using local profiles. The weather data, soil properties, and heating load profile were modified to make the model suitable for application in China. Typical meteorological year data generated from Meteonorm [44] were used as the yearly weather data for the four locations.

A five-floor residential building with 12 family apartments on each floor was analyzed based on a typical local residential building. The selected building was developed in Sketchup [45]. The thermal characteristics of the building envelopes, personnel occupancy rate, lighting utilization rate, and equipment utilization rate were assumed according to the Chinese design standard for residential buildings [46,47]. A community comprising eight typical residential buildings with a total heated area of 33,600 m² was simulated to quantify the hourly heating in each location. The heating load profile at each location was acquired by simulating the building model in TRNSYS using local weather data with an indoor cut-off temperature of 18 °C [46,47]. The building model, design characteristics, and soil properties at the four locations are presented in Supplementary materials. The hourly and cumulative heating loads at the four locations are presented in Fig. 5. Note that only space heating was considered. Domestic hot water (DHW) was excluded because there is hardly a central supply system for it in the built environment in China.

3.3. Adaptive measures

Adaptive measures were introduced to the system design to meet the local climate and heating load profiles at the four locations, including the solar collector tilt angle, solar collector area, short-term storage tank volume, and borehole number. Different solar collector tilt angles were tested, and the most favorable angle was selected. Furthermore, the solar collector area was determined by considering an oversizing of 20% of the heating load to cover peak demands [48]. Additionally, the borehole number for each location was revised based on the heating load relative to the DLSC system. The short-term storage tank volume was calculated based on the solar collector area and solar intensity according to Ref. [49]. The adaptive system configurations for the four locations are summarized in the Supplementary materials.

4. Results

This section summarizes the findings from model validation, techno-economic-environmental analysis, parametric study, and optimization.

4.1. Model validation

The annual energy flows and the SFs of the TRNSYS model developed

Table 2
Climatic conditions of the four locations.

	Unit	Harbin	Urumqi	Shanghai	Chengdu
Climate		Temperate monsoon climate	Temperate continental climate	Subtropical monsoon climate	Monsoon-influenced humid subtropical climate
Latitude	°	45	43	31	30
HDD18	°C·day	5032	4329	1540	1344
Average temperature	°C	5.5	8.0	17.5	17.4
Average GHI	W/m^2	151	164	145	113
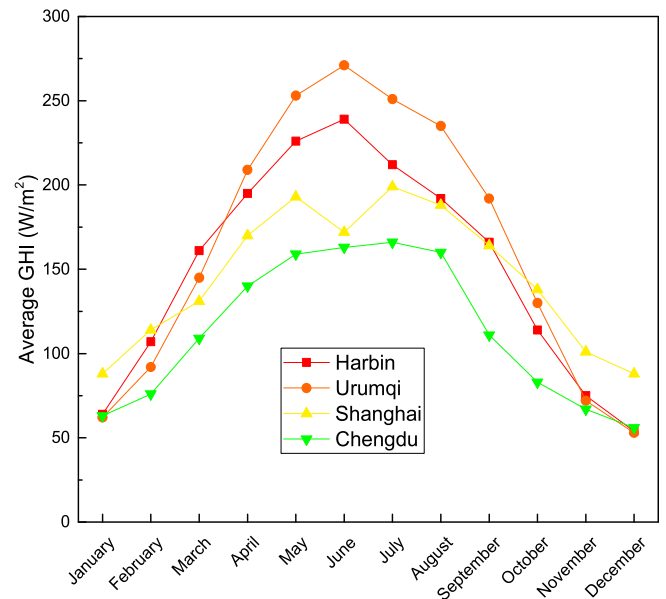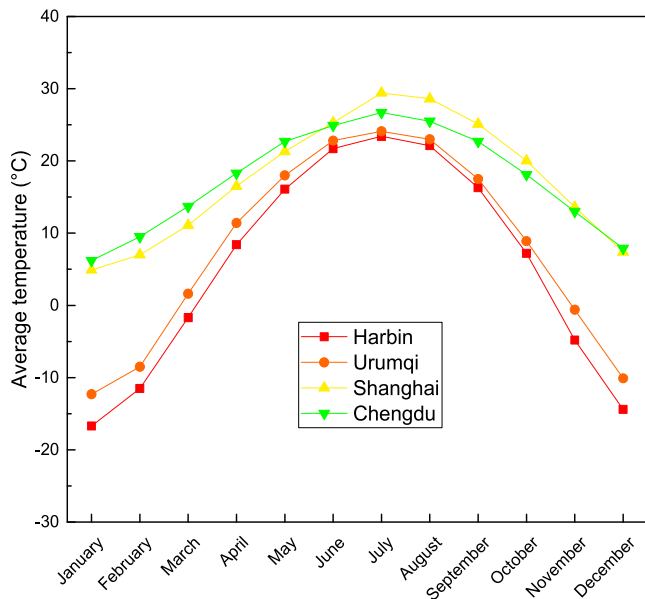
Fig. 4. Monthly average temperature and GHI at the four locations.

in this study were compared with those of the DLSC measurements, DLSC simulation results, and two previous simulation results of the DLSC system (Renaldi's [50] and Flynn's [51]), as shown in Fig. 6. The energy flows and SFs of the developed TRNSYS model, DLSC measurements, Renaldi's, and Flynn's were performed from July 1, 2007, to June 30, 2012, while those of the DLSC simulation were performed from January 1, 2007, to December 30, 2012.

Generally, the developed TRNSYS model agrees with the trend of DLSC measurements. The different solar irradiation sources can explain the differences in the annual solar energy collected. The solar irradiation adopted in the TRNSYS model was satellite-based data, whereas the DLSC measurements were based on ground-measured data. Although the solar irradiation used in the developed TRNSYS model was corrected according to the DLSC measurement, the correction was based on a year-level while the simulation ran in a timestep of 10 min. The differences in energy flow charging to and discharging from the borehole are attributable to the modifications made throughout the years. As described by Sibbitt et al. [52], the implementation of system modifications and controls allowed the system to operate in accordance with the design. The modifications in the district loop temperature control settings can also explain the differences in solar energy to load and total energy to load. Moreover, the limitation of the load correction can also partially explain the differences.

Table 3 summarizes the differences compared with the DLSC measurements among the different simulation results. The mean difference of the developed TRNSYS model is lower than that of the other sources, which indicates that the developed TRNSYS model has sufficient accuracy for implementation in the examined locations.

4.2. Performance evaluation

This section presents the technical, economic, and environmental performances of implementing STES at the four examined locations.

4.2.1. Technical performance

The representative energy flows at the four locations are shown in Fig. 7. A decreasing trend is observed in the figure of solar energy collected, which can be explained by the fact that more thermal energy is needed to charge the borehole during the first few years. More heat is charged into the borehole, and less heat is discharged to reach a thermal balance in the early years. Therefore, a decreased energy flow to the borehole and an increased energy flow from the borehole were observed. Since the borehole stores more heat during operation, the solar energy to the load increases over time, and the energy flow from the boiler to the load decreases accordingly. The total energy to load is stable because the same heating load profile is used yearly. Besides, since the Harbin case comprises the highest heating load, the energy flows are the largest compared with the other cases. It should be noted that more heat is charged into the borehole in the Harbin case; however, less heat is discharged from the borehole than in the Urumqi case, which can be explained by the higher heat loss of the borehole in the Harbin case because of the larger borehole volume, higher soil thermal diffusivity, and cold climate. The energy flows of the Chengdu case were the lowest because the Chengdu case has the lowest heating load. However, the energy flow from the boiler to the load is higher in the Chengdu case than in the Shanghai case, primarily owing to the low solar irradiation in the Chengdu case; therefore, more heat from the boiler is required to meet the heat demand.

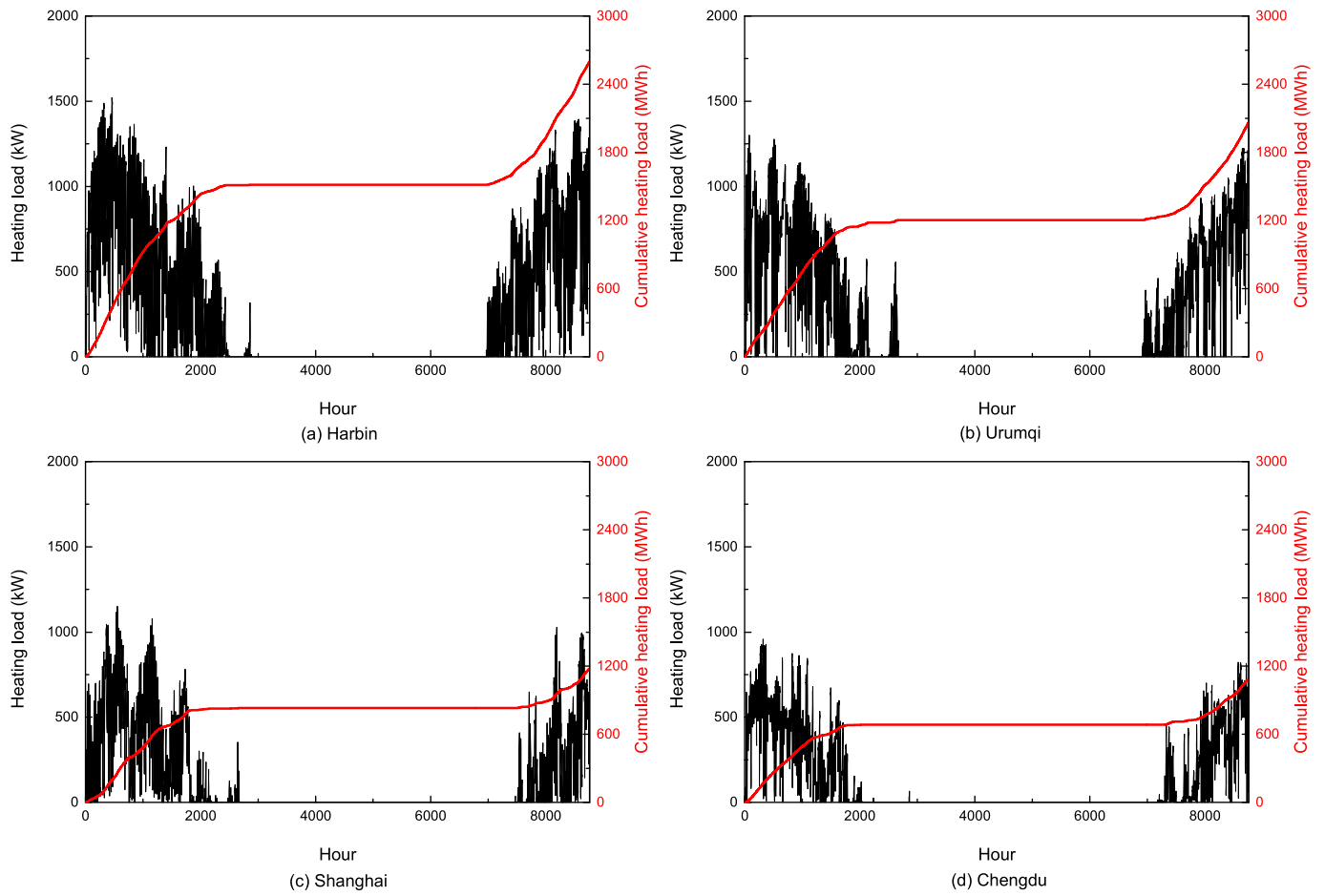Fig. 8 illustrates the SFs and storage efficiencies at the four locations.

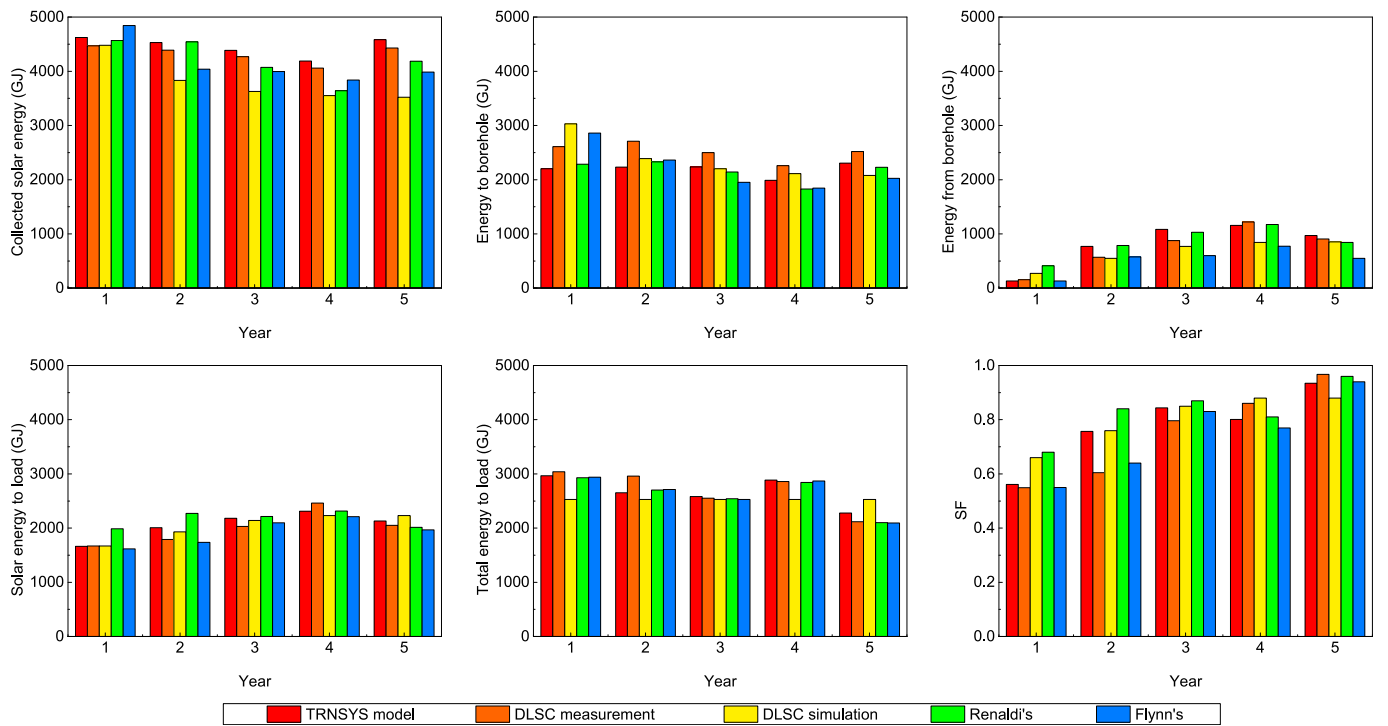**Fig. 5.** Heating load profiles at the four locations.

Fig. 6. Energy flows and SFs during the first five years of operation from different sources.

Table 3
Differences between different simulation results and DLSC measurements.

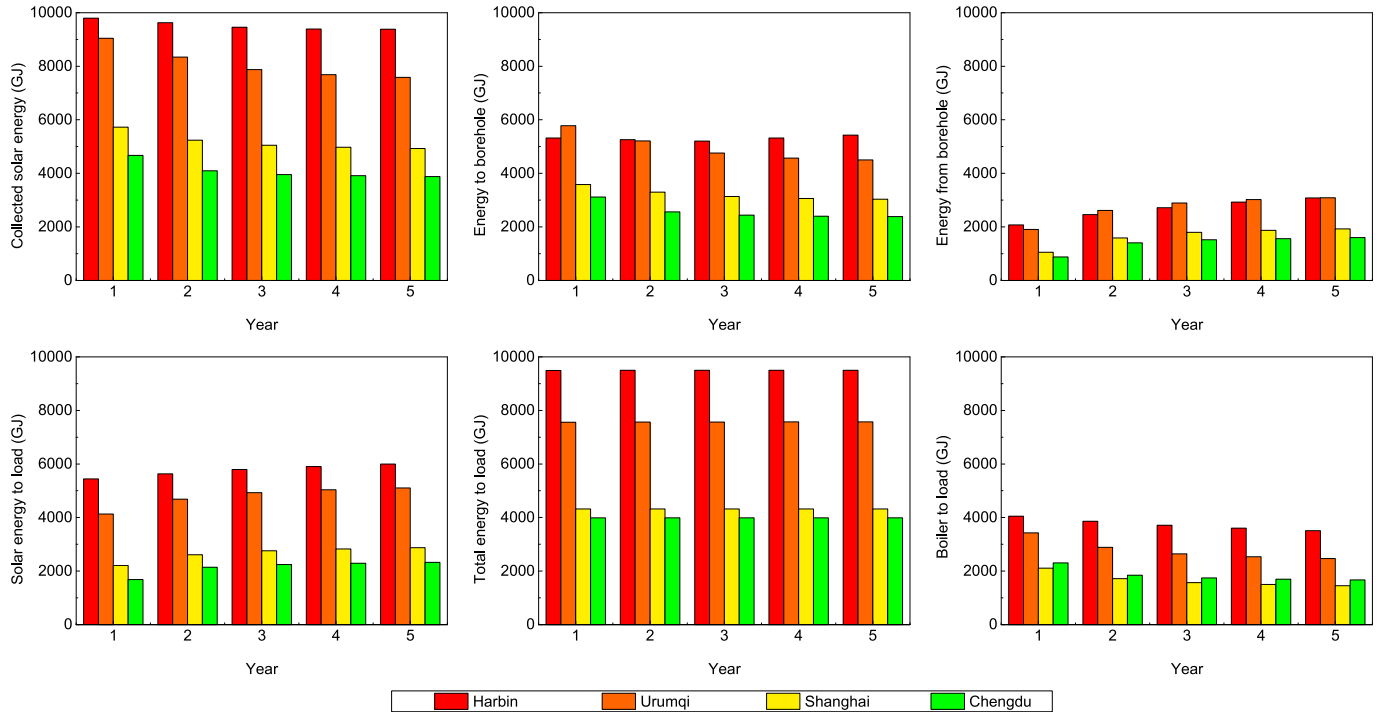| Source	Collected solar energy	Energy to borehole	Energy from borehole	Solar energy to load	Total energy to load	SF	Mean difference
TRNSYS model	3.2%	12.9%	17.2%	6.0%	4.5%	8.7%	8.8%
DLSC simulation [53]	12.2%	12.8%	25.3%	6.3%	12.6%	12.8%	13.7%
Renaldi's [50]	5.2%	14.3%	46.2%	12.5%	2.9%	15.7%	16.1%
Flynn's [51]	7.7%	16.5%	25.1%	4.8%	2.9%	4.7%	10.3%

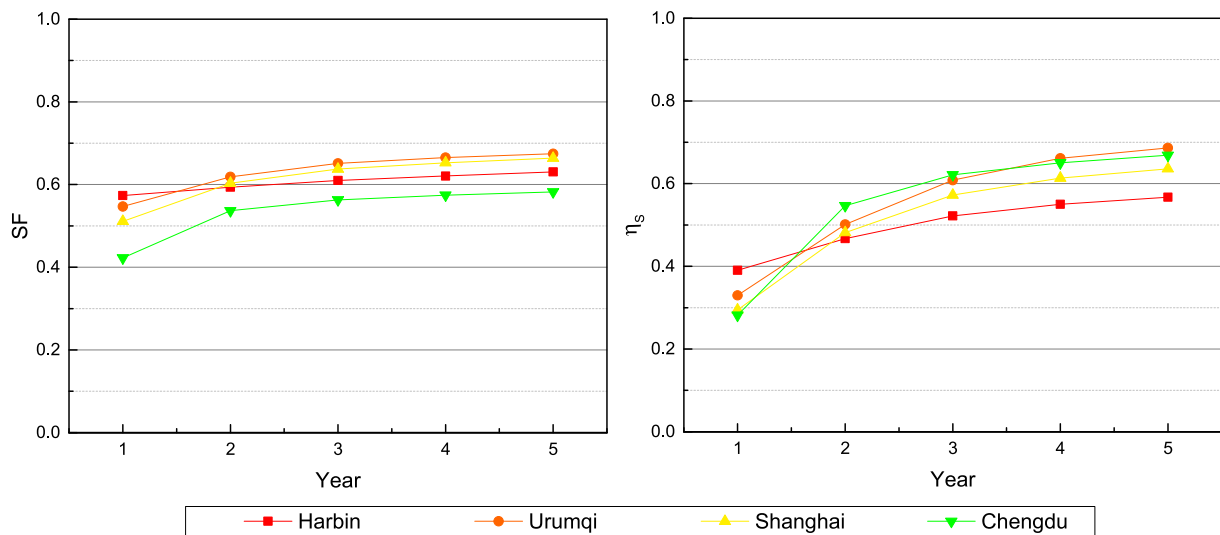**Fig. 7.** Energy flows of the STES systems at the four locations.

Fig. 8. SFs and storage efficiencies of the STES systems at the four locations.

The SFs and storage efficiencies have a faded growth trend because the borehole gradually reaches a thermal balance during operation. Since the Urumqi case has an abundance of solar resources than other locations, it has the highest SF and storage efficiency. The SF in the Chengdu case is the lowest owing to the low solar irradiation in the area. Notably, in the Harbin case, both the SF and storage efficiency are the highest in the first year of operation; however, the other cases gradually exceed figure. It is because the borehole is preheated to 25 °C, and the Harbin case has the largest borehole volume; therefore, initially, the Harbin case stores the most thermal energy. However, the high heat loss of the borehole caused by the cold climate and high soil thermal diffusivity slows the growth trend.
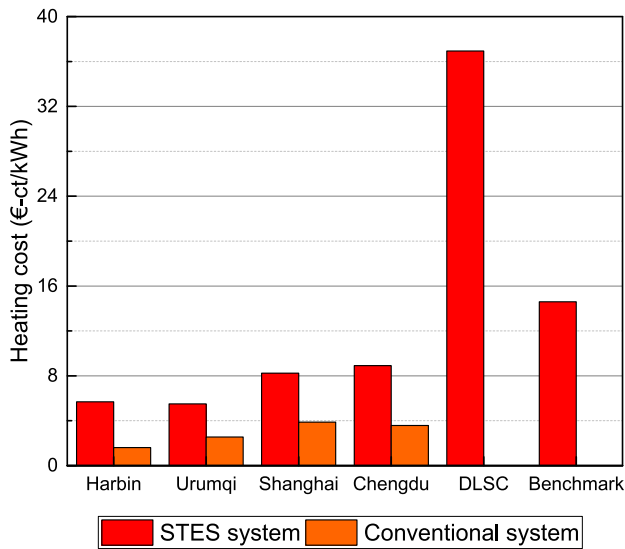
Fig. 9. Heating costs of the STES and conventional systems at the four locations, the DLSC system, and the benchmark case in Europe (Calculation process presented in Supplementary materials).

4.2.2. Economic performance

Economic performance was evaluated through LCOH analysis and comparison. Fig. 9 shows the LCOH of the proposed STES systems at the four locations. Identical equipment unit prices were used for different cases, and the electricity and natural gas prices were location-based. It was found that the Urumqi case achieves the lowest heating cost owing to its cheaper electricity and natural gas price than the other locations. The Chengdu case has the highest heating cost owing to its low solar irradiation. There was no significant difference in LCOH in a similar climate zone. In summary, the STES system is more attractive in the northern area with a higher heating load and better solar irradiation than in the southern region.

The heating costs of the conventional systems were also calculated to position the STES project in the local heat energy market. The calculations were based on a coal-fired combined heat and power (CHP) system for the Harbin case and a natural gas-fired CHP for the Urumqi case. For the Shanghai and Chengdu cases, it was assumed that air conditioning systems supplied heat to the proposed community because air conditioning systems account for the highest share of the most common household heating devices in southern China [54]. Fig. 9 compares the heating costs of the STES and conventional systems at the four locations. It was found that the heating cost of the STES system in Harbin was more than three times that of the coal-fired CHP. The heating cost of the STES system in Urumqi is more than twice that of the natural gas-fired CHP. The heating costs of the STES systems in Shanghai and Chengdu were more than twice those of air conditioning systems. It is evident that STES cannot compete with existing fossil-fuel-dominated heating supply technologies. Currently, individual heating in the southern area is more expensive than DH in the north.

Furthermore, the heating costs of the STES systems at the four locations were also compared with those of the DLSC system and the benchmark case in Europe, as shown in Fig. 9. The benchmark case in Europe was based on the STES with solar heating presented by the International Energy Agency Solar Heating and Cooling program, indicating the average heating cost of 14 practice examples in operation in Europe [55]. The costs of the examined STES projects were converted to 2021 constant prices in Euros using the inflation and exchange rates derived from the Organization for Economic Co-operation and Development [56,57]. It was found that the implementation of the STES system in China has a lower LCOH, primarily because of the low-priced equipment and labor. Meanwhile, the LCOH of the DLSC system is much
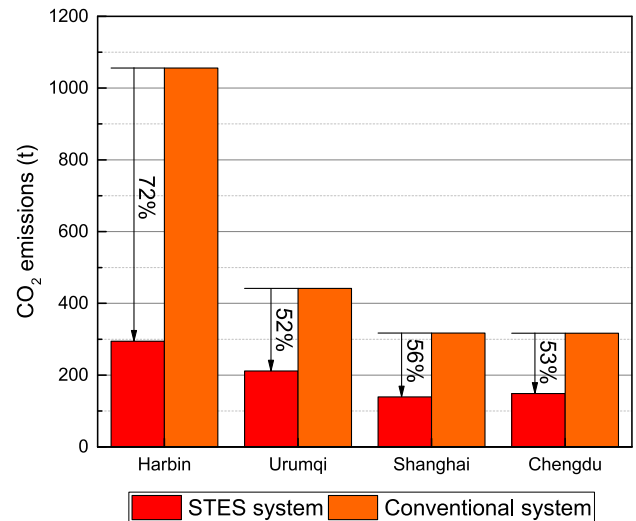

Fig. 10. CO_2 emission saving of the STES systems at the four locations. (Calculation process presented in Supplementary materials).

higher than that of the other cases because it was designed to achieve over 90% SF; namely, the system is oversized.

4.2.3. Environmental performance

The CO_2 emission saving of the STES systems at the four locations is illustrated in Fig. 10. Compared with the existing heating system, the implementation of the STES has the potential to reduce CO_2 emissions at all the examined locations. The Harbin case has the highest reduction potential since 95.8% of the existing DH system is based on coal combustion [58]. The Urumqi case reduces the least CO_2 emissions, primarily because natural gas dominates the existing DH system [59].

4.3. Parametric study and optimization

This section summarizes the findings from a parametric study investigating how the system configurations influence the overall performance, a sensitivity analysis on the LCOH calculation, and a multi-objective optimization considering economic feasibility and environmental impact.

4.3.1. Parametric study

Several system configurations were further investigated to determine the impact on the technical, economic, and environmental performance and provide a solid base for the following optimization, including solar collector area, short-term storage tank volume, and borehole number. Accordingly, SF, LCOH, and CO_2 emission savings were utilized as indicators, and the Harbin case was used to perform the parametric study.

The SFs, LCOHs, and CO_2 emission savings for various solar collector areas are shown in Fig. 11. The SF increases as the solar collector area increases. However, the increased extent decreases because more solar energy collected through the larger solar collector area can cause a higher temperature of the borehole, leading to greater heat loss. In addition, the SF trends of different solar collector areas are similar; however, a higher solar collector area leads to a more rapid increment in the early years. It is primarily because more heat collected owing to a larger solar collector area helps speed up the warm-up process of the borehole. As the solar collector area increased, the LCOH decreased when the solar collector area was lower than 4870 m^2 but increased subsequently. The decreasing trend is because more solar energy is harvested to supply the load, which corresponds to less natural gas usage. However, as the solar collector area increases, the benefits of more solar energy collected cannot offset the impact of increased investment in the LCOH; therefore, the LCOH starts to increase. It
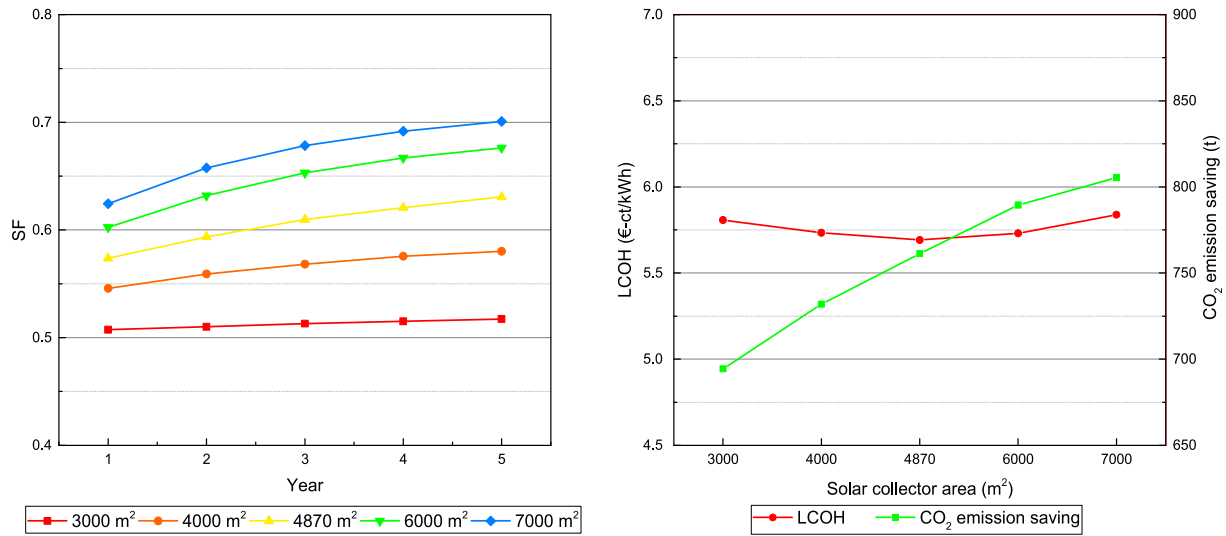
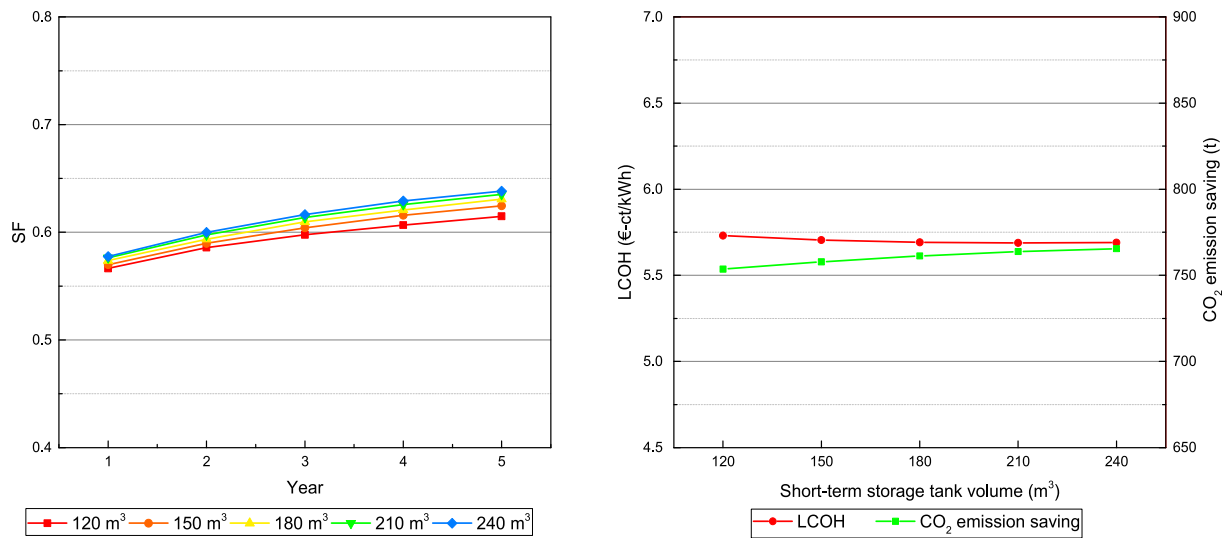**Fig. 11.** SFs, LCOHs, and CO$_2$ emission savings for various solar collector areas.

Fig. 12. SFs, LCOHs, and CO$_2$ emission savings for various short-term storage tank volumes.
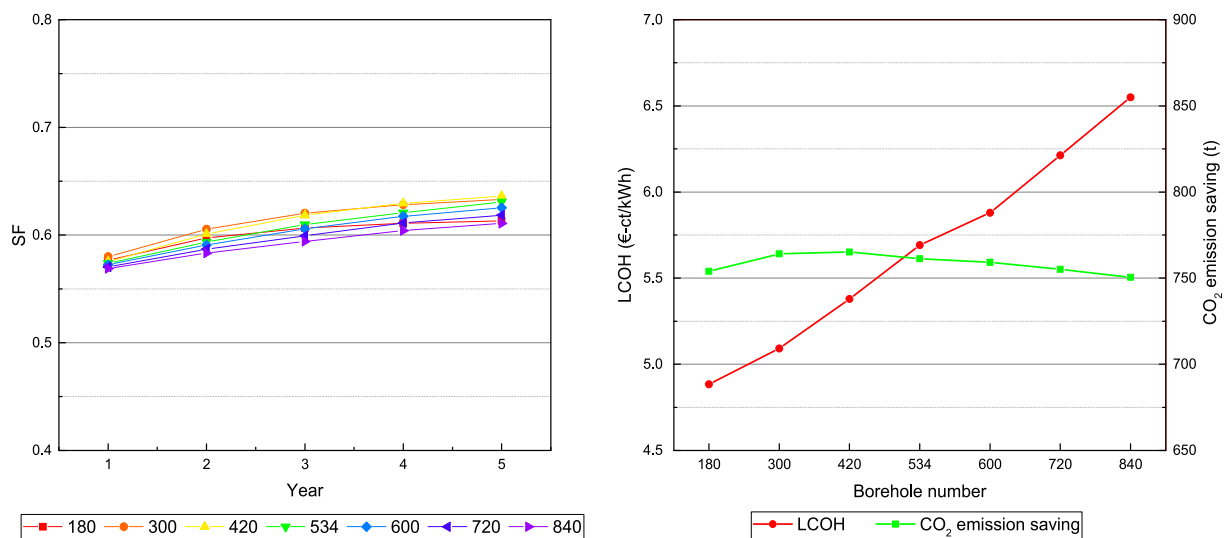

Fig. 13. SFs, LCOHs, and CO$_2$ emission savings for various borehole numbers.

highlights the significance of choosing an appropriate solar collector area to achieve the lowest LCOH. The blind pursuit of a high SF has a negative impact on economic performance. In addition, the STES system reduces more CO_2 emissions as the solar collector area increases. The increased rate of CO_2 emission savings was found to decrease. The trend also agrees with the previous analysis of SF.

The SFs, LCOHs, and CO_2 emission savings for various short-term storage tank volumes are presented in Fig. 12. It was found that the short-term storage tank volume had less influence on the system performance than the solar collector area. A larger short-term storage tank volume helps increase SF slightly and reduce more CO_2 emissions. Since enlarging the short-term storage tank allows to store more heat in the buffer, additional solar thermal energy will be transferred to the load directly, leading to less heat loss caused by long-term storage. In addition, with an increment in the short-term storage tank volume, the influence on the performance gradually decreases, similar to the tendency of the solar collector area. A turning point of the LCOH was found for the same reason as the solar collector area.

Fig. 13 illustrates the SFs, LCOHs, and CO_2 emission savings for various borehole numbers. As the borehole number increases, the SF increases until the borehole number is less than 420 and decreases afterward because increasing the borehole number helps store more thermal energy. However, an oversized borehole can cause more heat loss. Additionally, borehole investment accounts for the highest proportion of the total investment; therefore, increasing the borehole number can rapidly increase the LCOH. Since the borehole number is less influential on the SF but has a larger impact on the LCOH, it is possible to reduce it to achieve a lower LCOH. Moreover, increasing the borehole number helps reduce more CO_2 emissions because more heat can be stored owing to the larger storage size. However, unduly increasing the borehole number negatively affects the reduction of CO_2 emissions because a higher borehole volume can reduce the borehole storage temperature. Consequently, the boiler needs to consume more natural gas to increase the temperature to meet the supply setpoint temperature.

4.3.2. Sensitivity analysis

A sensitivity analysis based on the Harbin case was conducted to investigate the influence of the equipment unit prices, discount rate, and electricity and natural gas prices on the LCOH calculation. The fifth-year results were used in the calculation because the BTES system develops its maximum capacity for energy contribution from the fifth year of operation [48]. Fig. 14 presents what effect 5% and 10% increase or decrease in investment cost, fuel cost, and discount rate value will have on the LCOH of the STES system. Note that the unit price of the borehole, solar collector, and pipeline are influential factors in the LCOH of the STES system among the investment costs. The LCOH is more sensitive to the natural gas price than electricity. The discount rate also has a significant impact on the LCOH calculation. Considering that the natural gas price and discount rate are locally based, cheaper solar collectors and pipelines and more efficient borehole construction can reduce the LCOH of the STES system.

4.3.3. Multi-objective optimization

The parametric study found that the solar collector area and borehole number are the most influential variables in the system configurations; therefore, they were selected as the main variables in the optimization. Fig. 15 (left) presents the Pareto fronts of the four cases through multi-objective optimization. These curves demonstrate the non-dominated solutions where minimum LCOH and CO_2 emissions occur. The LCOH increased when CO_2 emissions decreased, and the opposite trend was observed. The CO_2 emission increased when the LCOH was reduced. For comparison, the conventional heating options at the four locations are presented in Fig. 15 (left). The proposed STES systems at the four locations fail to compete with conventional heating options in terms of cost. However, they certainly have a positive influence on the environment.

Upon identifying the Pareto front, it is critical to select a solution from the Pareto front by following the wills and needs of the stakeholders [60]. Therefore, the CO_2 avoidance costs of the four cases were calculated based on the set of non-dominated solutions on the Pareto fronts, as shown in Fig. 15 (right). Accordingly, the Harbin achieved the lowest CO_2 avoidance cost at the same SF value. It also has the highest CO_2 avoidance potential because the conventional heating option is coal-fired CHP. Besides, Chengdu's highest CO_2 avoidance cost at the same SF value is due to its weak solar resources. Larger system size is
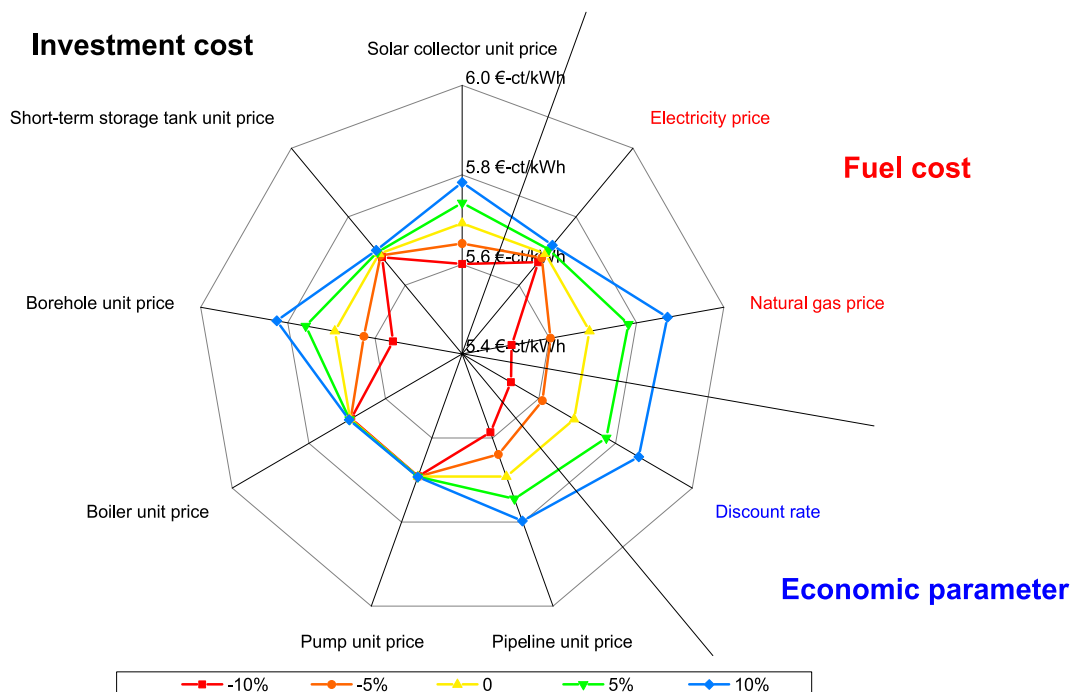

Fig. 14. Sensitivity analysis of the LCOH calculation with 5% and 10% increase or decrease in investment cost, fuel cost, and discount rate.
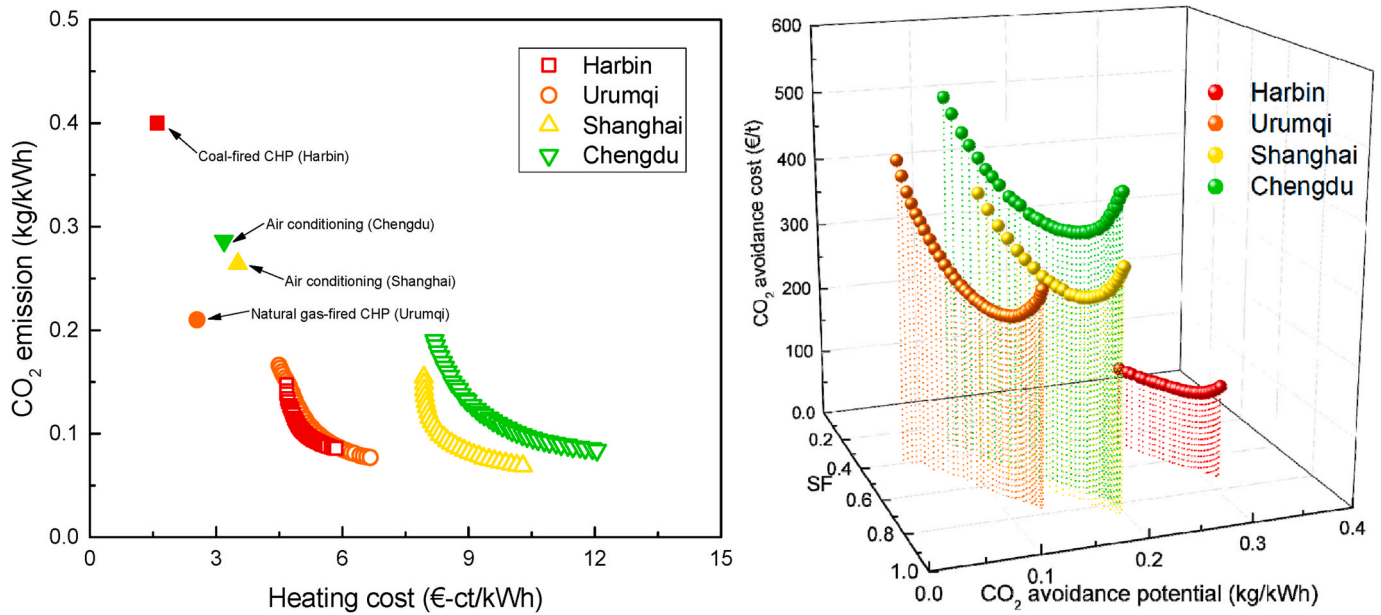
Fig. 15. Pareto fronts (left) and CO_2 avoidance costs (right) of the four cases.

Table 4
System configurations and techno-economic-environmental performances of the optimal solutions for the four cases (compared with the original design).

	Unit	Harbin	Urumqi	Shanghai	Chengdu
Solar collector area	m²	5000 (3%)	5000 (12%)	4500 (39%)	5000 (14%)
Borehole number		150 (−72%)	330 (−23%)	240 (0%)	270 (22%)
SF	%	60.8 (−4%)	66.7 (−1%)	75.8 (14%)	64.3 (10%)
Storage efficiency	%	69.2 (22%)	70.5 (3%)	60.5 (−5%)	66.6 (0%)
LCOH	€-ct/kWh	4.9 (−15%)	5.4 (−2%)	8.5 (3%)	9.3 (4%)
CO_2 emission saving	t/a	752.5 (−1%)	228.5 (−1%)	205.0 (15%)	183.2 (9%)
CO_2 emission saving per heat	kg/MWh	285.1 (−1%)	108.7 (−1%)	170.6 (15%)	165.4 (9%)
CO_2 avoidance cost	€/t	114.4 (−19%)	260.8 (−3%)	291.4 (−9%)	368.3 (−2%)

needed to achieve the same level of the SF as in the other cases, namely, higher costs. The Urumqi case has the lowest CO_2 avoidance potential since its conventional heating option is a natural gas-fired CHP with a lower CO_2 equivalent emission factor.

The optimal solutions for the four cases were selected with the minimum CO_2 avoidance cost criteria. Table 4 lists the system configurations and techno-economic-environmental performances of the optimal solutions for the four cases. Compared with the original design, it was found that the pathway of optimization in the cold climate zone (Harbin and Urumqi) involves reducing the borehole number to reach a higher storage efficiency and lower LCOH while reducing less CO_2 emissions. The optimization pathway for the warm climate zone (Shanghai and Chengdu) involves increasing the solar collector area to increase the SF and reduce more CO_2 emissions, although the LCOH slightly increases. Moreover, the soil properties should be considered when designing the borehole number. For instance, in the two cases in the cold climate zone, the borehole number of the Urumqi case is more than twice that of the Harbin case because the soil thermal diffusivity of the Harbin case is higher than that of the Urumqi case. Significant heat loss can occur in the cold climate zone if the thermal diffusivity of the soil is high. Thus, reducing the borehole number for cases with high soil

thermal diffusivity can help increase the storage efficiency of the borehole. Besides, the specific heat capacity of the Urumqi case was also lower than that of the Harbin case. Notably, increasing the borehole number for cases with a low specific heat capacity can help decrease the borehole temperature and reduce the heat loss accordingly. Within the two cases in the warm climate zone, the borehole number of the Chengdu case is higher than that of the Shanghai case because the specific heat capacity of the Chengdu case is lower than that of the Shanghai case.

5. Discussion

This study performed a techno-economic-environmental analysis of applying STES with solar heating in different climate zones of China based on the developed TRNSYS model. There are underlying assumptions in the TRNSYS model that influence model accuracy. For instance, the borehole component (type 557a) assumes that boreholes are uniformly placed within a cylindrical storage volume of the ground. In addition, it only considers the conductive heat transfer between the pipes and soil, that is, it ignores the groundwater flow. The storage efficiency decreases with the presence of groundwater flow [61]. A lower storage efficiency leads to a lower SF and more gas consumption from the gas boiler, negatively impacting the technical, economic, and environmental performance of STES. Some studies have used detailed modeling software for boreholes (for example, Ground Heat Exchanger Analysis, Design and Simulation) to provide flexibility in the borehole layout design and produce more favorable results in borehole simulations [62,63]. Nevertheless, TRNSYS has been widely used in STES modeling and has been proven to exhibit a good level of accuracy [64, 65].

More accurate weather data, heating load profiles, and more suitable model components were used in this study to obtain a better validation result. Consequently, the difference between the simulation results of this study and the DLSC measurements remained within 10%. It indicates that the model is sufficiently accurate for predicting the performance of subsequent implementations. Moreover, the soil properties of the examined locations chosen in this study were derived from peer-reviewed journal articles, indicating their potential values in these locations. Since soil properties affect the technical performance of the STES system, especially the storage efficiency [50,66], in situ thermal response tests (TRT) from practical engineering are required to improve

the accuracy of the performance prediction [67,68].

This study developed an STES model based on the DLSC schematic design. The model was validated with the DLSC measurements and previous simulation results, and the system size was adapted to be allocated in different climates. The limitation of the solar thermal collector and borehole installation was not considered. Applying a uniform system structure in the four case studies enabled quantifying the impact of local context (climate conditions and existing heating infrastructure) on the optimal configuration planning, techno-economic-environmental performance, and feasibility of the STES application. Conclusions on the key technical parameters in achieving the optimal techno-economic-environmental performance and determining the configuration planning of STES in different climate zones were drawn by comparing the optimal configuration and the original design. DHW was excluded in this study since there is no central DHW supply in the conventional system. However, adding DHW has a positive impact on solar energy integration. It is suggested to be included in future sustainable heating systems.

STES with solar heat can reduce fossil fuel consumption and CO_2 emissions, facilitating the clean heating transition. It can also be beneficial to other low-cost sources, including industrial waste heat and waste heat from CHP-based power generation outside the heating season. Besides working as the heat supply unit, STES can be integrated with heat pumps, taking advantage of low-temperature heat sources during the summer and leading to a high coefficient of performance (COP) of heat pumps. Coupling with power-to-heat technologies can increase the utilization of renewable power sources and provide electrical network balancing [3].

In northern China, DH systems primarily use fossil-based boilers and CHP plants (in which coal-based heat supply units accounted for 92% of the total [54]). A series of national development plans have encouraged clean fossil-based DH, and carbon capture and storage (CCS) is regarded as a potential method. According to the Intergovernmental Panel on Climate Change [69], the total costs for CO_2 capture, transport, and geological storage are approximately 30–71 \$/t and will cause a 20–30% loss in plant efficiency; the corresponding cost will increase by 40–80%. Carbon capture costs will be higher in the upfront installation costs of CCS equipment because CCS-related devices are not installed in traditional coal-based plants in China [70]. Therefore, the heating cost of the STES application may be slightly higher than that of the coal-based heating options combined with CCS. However, it can help increase the share of renewable energy in DH systems.

Electricity-based heating solutions are commonly used in southern China, among which air conditioning and electric heaters are prevalent [54]. According to *China's national economic and social development statistics bulletin* in 2020, China's installed power generation capacity is 2200 GW with 56.6% thermal power, 16.8% hydropower, 24.3% renewable power, and 2.3% nuclear power [71]. The ratio of thermal power is expected to decrease to 46.8% by 2025 [72]. The development of renewable power may reduce the advantage of STES in terms of CO_2 emission reductions compared to conventional heating systems in the south. The carbon intensity of the electricity generation sectors needs to be reduced by 66% and 62%, respectively, to make the CO_2 emission level of the conventional heating in Shanghai and Chengdu comparable with the STES system. The cost of decarbonizing China's power sector through wind and solar power is between 19 and 31€/t [73], which is cheaper than STES (291–368 €/t). Therefore, for clean heat transition in southern China, decarbonizing the power sector is more economically attractive than STES.
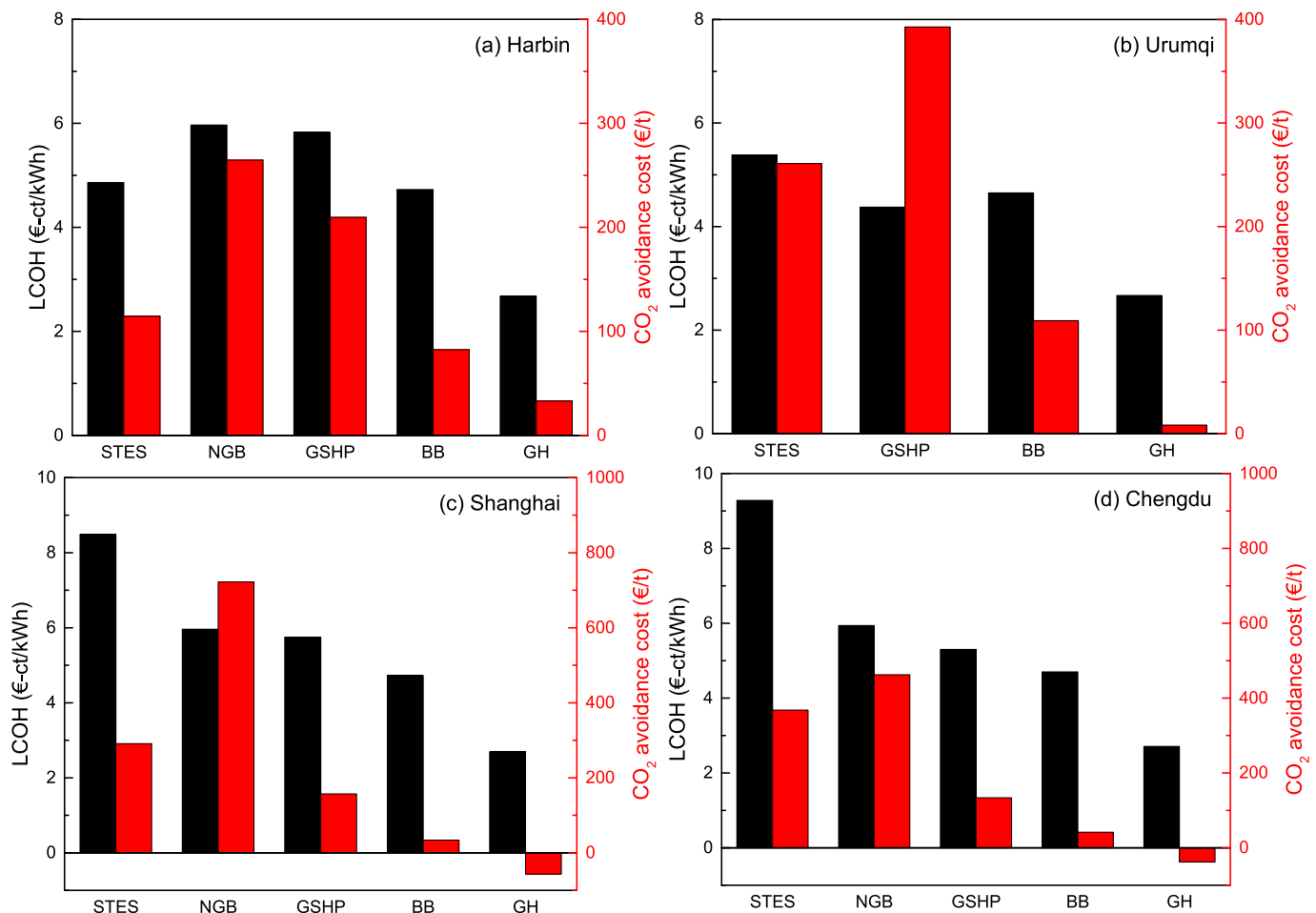

Fig. 16. LCOHs and CO_2 avoidance costs of the sustainable heating options in the four locations.

Some studies have investigated the economic and environmental performance of sustainable heating options replacing coal-based heating in the Chinese context, including NGBs [74], ground source heat pumps (GSHPs) [75], biomass boilers (BBs) [74], and geothermal heating (GH) [76]. Fig. 16 compares the LCOHs and CO_2 avoidance costs of the STES and the sustainable heating options. The cost and emission data were derived from the previous studies and adopted based on the local context in the four locations. It is evident that GH has the lowest LCOH and CO_2 avoidance cost, especially in Shanghai and Chengdu, where it has a lower LCOH than the conventional system and emits less CO_2; however, the application partially depends on the suitability of local geological conditions. BB also has a relatively low LCOH and CO_2 avoidance cost. Still, the limited availability of biomass resources should be aware, and biomass is also needed in other sectors to support decarbonization transitions. STES has lower CO_2 avoidance costs than GSHP in the two northern locations. In comparison, it has higher CO_2 avoidance costs than GSHP in the two southern locations, indicating STES is attractive in northern areas, and GSHP is attractive in southern regions.

6. Conclusions

STES combined with DH positively impacts clean heat transition. Literature study shows a lack of in-depth insights into economic and environmental performances to provide the facts on the position of STES applications compared with other sustainable heating technologies. An optimization approach is needed to obtain insights into the optimal economic and environmental performance and the conditions to achieve it. It requires an integrated optimization criterion and method to select the optimal solution. This study develops a comprehensive quantitative method for the techno-economic-environmental performance analysis and proposes an integrated optimization criterion by including economic and environmental impacts to perform a multi-objective optimization on STES system configurations. The impact of local context on the optimal configuration planning, techno-economic-environmental performance, and feasibility of the STES application is examined. The key technical parameters in achieving the optimal techno-economic-environmental performance and determining the configuration planning of STES in different climate zones are investigated. The position of STES compared to other sustainable heating options considering the local context is identified. The TRNSYS modeling tool is adopted to analyze the performance of the STES systems, and Pareto optimization is applied to treat the multi-objective optimization. This study provides a comprehensive and transparent showcase highlighting the importance of the local context in determining the feasibility of STES in the clean heating transition.

From a technical perspective, the four examined locations can potentially implement the STES system. During the operation, the energy flows of solar energy collected, energy to the borehole, and boiler to load decreased, while energy from the borehole and solar energy to load increased. The SFs and storage efficiencies had a faded growth trend. The Urumqi achieved the highest SF and storage efficiency. The SFs and storage efficiencies of the four case studies ranged between 58-67% and 57–69%, respectively, which are fairly similar in very different climates. It was found that implementation in locations with higher solar irradiation and heat retention of soil can achieve higher SF and storage efficiency. From an economic point of view, the Urumqi case achieved the lowest heating cost among the four case studies (5.4–8.7 €-ct/kWh). However, the heating costs of the STES systems in all examined locations were more than twice those of the conventional system (fossil fuel-based CHP for Harbin and Urumqi and air conditioning for Shanghai and Chengdu). Compared with the DLSC project and the benchmark case in Europe, the LCOH of STES applications in China is one to three times lower. From an environmental perspective, the STES system is the most attractive in Harbin to replace the conventional coal-based DH system (72% CO_2 emission saving). Implementing the STES system in the other

three locations also has a large potential to reduce CO_2 emissions (52–56%). The CO_2 avoidance cost of the four case studies ranges between 114 and 368 €/t. Harbin achieved the lowest CO_2 avoidance cost because the conventional heating option is coal-fired CHP. Chengdu's highest CO_2 avoidance cost is due to its weak solar resources. In summary, implementing the STES system in China is technically feasible. It is attractive in locations with rich solar resources, high heating loads, and currently coal-based heating systems.

The parametric study shows that a larger solar collector area and short-term storage tank volume help increase SF and reduce more CO_2 emissions. A turning point was found in the LCOH trend, indicating the significance of choosing an appropriate size to achieve the lowest LCOH. A larger borehole number can cause an increase in the LCOH, while a turning point was found in the SF and CO_2 emissions trends. Since the borehole number is less influential on the SF but has a larger impact on the LCOH, it is possible to reduce it to achieve a lower LCOH. The parametric study highlights that the solar collector area has a more significant impact on the SF and CO_2 emission reduction, and the borehole number has a greater influence on the LCOH, while the short-term storage tank is less influential than those two parameters. Besides, the sensitivity analysis on the LCOH calculation shows that the unit price of the borehole, solar collector, and pipeline are influential factors in the LCOH of the STES system among the investment costs. The LCOH is more sensitive to the natural gas price than electricity. The discount rate also has a significant impact on the LCOH calculation. Moreover, the multi-objective optimization for minimizing LCOH and CO_2 emissions proposes that appropriately reducing the borehole number for the STES system in cold climate zones can help achieve a higher storage efficiency and a lower LCOH. Increasing the solar collector area in warm climate zones is conducive to achieving higher SF and greater CO_2 emission reduction. The soil properties should be considered when designing the borehole number.

For sustainable heat transition in China, STES helps increase the share of renewable energy in fossil fuel-based DH in the northern area. In southern China, where electric heating is the dominant heat supply, decarbonizing the power sector is more economically attractive than applying the STES system. Compared to other sustainable heating options, STES fails to compete with GH and BB, but their applications are limited by geological conditions and availability. STES has a lower expense for obtaining environmental benefits than NGB and GSHP in the northern area, while GSHP is more attractive than STES in the southern region. The focus of this study is STES. For future research, it is suggested to carry out an integrated assessment of the technical, economic, and environmental performances of various sustainable heating technologies and their implementation feasibility at the local level. This way, STES with solar heating will be assessed in a broad context in which locally available sustainable heat options are included.

CRediT authorship contribution statement

Tianrun Yang: Conceptualization, Methodology, Software, Validation, Formal analysis, Investigation, Data Curation, Writing - Original Draft, Visualization. **Wen Liu**: Conceptualization, Investigation, Writing - Review & Editing, Supervision. **Qie Sun**: Investigation, Writing - Review & Editing. **Weihao Hu**: Investigation, Writing - Review & Editing. **Gert Jan Kramer**: Conceptualization, Writing - Review & Editing, Supervision.

Declaration of competing interest

The authors declare that they have no known competing financial interests or personal relationships that could have appeared to influence the work reported in this paper.

Data availability

Data will be made available on request.

Acknowledgments

Appendix A. Supplementary data

Supplementary data to this article can be found online at https://doi.org/10.1016/j.energy.2023.128389.

References

[1] Lund H, Østergaard PA, Connolly D, Mathiesen BV. Smart energy and smart energy systems. Energy 2017;137:556–65. https://doi.org/10.1016/j.energy.2017.05.123.

[2] Lund H, Østergaard PA, Connolly D, Ridjan I, Mathiesen BV, Hvelplund F, et al. Energy storage and smart energy systems. Int J Sustain Energy Plan Manag 2016;11(0):3–14. https://doi.org/10.5278/ijsepm.2016.11.2.

[3] Lyden A, Brown CS, Kolo I, Falcone G, Friedrich D. Seasonal thermal energy storage in smart energy systems: district-level applications and modelling approaches. Renew Sustain Energy Rev 2022;167:112760. https://doi.org/10.1016/j.rser.2022.112760.

[4] Lund H, Østergaard PA, Nielsen TB, Werner S, Thorsen JE, Gudmundsson O, et al. Perspectives on fourth and fifth generation district heating. Energy 2021;227:120520. https://doi.org/10.1016/j.energy.2021.120520.

[5] Yang T, Liu W, Kramer GJ, Sun Q. Seasonal thermal energy storage: a techno-economic literature review. Renew Sustain Energy Rev 2021;139:110732. https://doi.org/10.1016/j.rser.2021.110732.

[6] Guo F, Zhu X, Li P, Yang X. Low-grade industrial waste heat utilization in urban district heating: simulation-based performance assessment of a seasonal thermal energy storage system. Energy 2022;239:122345. https://doi.org/10.1016/j.energy.2021.122345.

[7] Yang T, Liu W, Kramer GJ, Sun Q. State of the art review of seasonal sensible heat storage. Energy Proc 2019;5:4255. https://doi.org/10.46855/energy-proceedings-4255.

[8] Mahon H, O'Connor D, Friedrich D, Hughes B. A review of thermal energy storage technologies for seasonal loops. Energy 2022;239:122207. https://doi.org/10.1016/j.energy.2021.122207.

[9] Dahash A, Ochs F, Janetti MB, Streicher W. Advances in seasonal thermal energy storage for solar district heating applications: a critical review on large-scale hot-water tank and pit thermal energy storage systems. Appl Energy 2019;239:296–315. https://doi.org/10.1016/j.apenergy.2019.01.189.

[10] Xu J, Li Y, Wang RZ, Liu W. Performance investigation of a solar heating system with underground seasonal energy storage for greenhouse application. Energy 2014;67:63–73. https://doi.org/10.1016/j.energy.2014.01.049.

[11] Kim M-H, Kim D, Heo J, Lee D-W. Techno-economic analysis of hybrid renewable energy system with solar district heating for net zero energy community. Energy 2019;187:1–19. https://doi.org/10.1016/j.energy.2019.115916.

[12] Salvestroni M, Pierucci G, Pourreza A, Fagioli F, Taddei F, Messeri M, et al. Design of a solar district heating system with seasonal storage in Italy. Appl Therm Eng 2021;197:117438. https://doi.org/10.1016/j.applthermaleng.2021.117438.

[13] Guo F, Zhu X, Zhang J, Yang X. Large-scale living laboratory of seasonal borehole thermal energy storage system for urban district heating. Appl Energy 2020;264:114763. https://doi.org/10.1016/j.apenergy.2020.114763.

[14] Semple L, Carriveau R, Ting DSK. A techno-economic analysis of seasonal thermal energy storage for greenhouse applications. Energy Build 2017;154:175–87. https://doi.org/10.1016/j.enbuild.2017.08.065.

[15] Huang J, Fan J, Furbo S. Demonstration and optimization of a solar district heating system with ground source heat pumps. Sol Energy 2020;202:171–89. https://doi.org/10.1016/j.solener.2020.03.097.

[16] Nilsson E, Rohdin P. Performance evaluation of an industrial borehole thermal energy storage (BTES) project – experiences from the first seven years of operation. Renew Energy 2019;143:1022–34. https://doi.org/10.1016/j.renene.2019.05.020.

[17] Liu L, Zhu N, Zhao J. Thermal equilibrium research of solar seasonal storage system coupling with ground-source heat pump. Energy 2016;99:83–90. https://doi.org/10.1016/j.energy.2016.01.053.

[18] Ciampi G, Rosato A, Sibilio S. Thermo-economic sensitivity analysis by dynamic simulations of a small Italian solar district heating system with a seasonal borehole thermal energy storage. Energy 2018;143:757–71. https://doi.org/10.1016/j.energy.2017.11.029.

[19] Tao T, Zhang F, Zhang W, Wan P, Shen X, Li H. Low cost and marketable operational experiences for a solar heating system with seasonal thermal energy storage (SHSSTES) in Hebei (China). Energy Proc 2015;70:267–74. https://doi.org/10.1016/j.egypro.2015.02.123.

[20] Launay S, Kadoch B, Le Métayer O, Parrado C. Analysis strategy for multi-criteria optimization: application to inter-seasonal solar heat storage for residential building needs. Energy 2019;171:419–34. https://doi.org/10.1016/j.energy.2018.12.181.

[21] Wang X, Zheng M, Zhang W, Zhang S, Yang T. Experimental study of a solar-assisted ground-coupled heat pump system with solar seasonal thermal storage in severe cold areas. Energy Build 2010;42(11):2104–10. https://doi.org/10.1016/j.enbuild.2010.06.022.

[22] Fiorentini M, Heer P, Baldini L. Design optimization of a district heating and cooling system with a borehole seasonal thermal energy storage. Energy 2023;262:125464. https://doi.org/10.1016/j.energy.2022.125464.

[23] Xiao X, Jiang Z, Owen D, Schrank C. Numerical simulation of a high-temperature aquifer thermal energy storage system coupled with heating and cooling of a thermal plant in a cold region, China. Energy 2016;112:443–56. https://doi.org/10.1016/j.energy.2016.06.124.

[24] Kubiński K, Ł Szabłowski. Dynamic model of solar heating plant with seasonal thermal energy storage. Renew Energy 2020;145:2025–33. https://doi.org/10.1016/j.renene.2019.07.120.

[25] Jiao Q, Liu W, Liu G, Zhang Y, Cai J, Qin H. Data measurement and analysis of a solar heating system with seasonal storage. Energy Proc 2015;70:241–8. https://doi.org/10.1016/j.egypro.2015.02.120.

[26] Yuan X, Heikari L, Hirvonen J, Liang Y, Virtanen M, Kosonen R, et al. System modelling and optimization of a low temperature local hybrid energy system based on solar energy for a residential district. Energy Convers Manag 2022;267:115918. https://doi.org/10.1016/j.enconman.2022.115918.

[27] Shah SK, Aye L, Rismanchi B. Multi-objective optimisation of a seasonal solar thermal energy storage system for space heating in cold climate. Appl Energy 2020;268. https://doi.org/10.1016/j.apenergy.2020.115047.

[28] IEA. District heating. https://www.iea.org/reports/district-heating;. [Accessed 19 March 2023].

[29] Zhou X, Xu Y, Zhang X, Xu D, Linghu Y, Guo H, et al. Large scale underground seasonal thermal energy storage in China. J Energy Storage 2021;33:102026. https://doi.org/10.1016/j.est.2020.102026.

[30] Li H, Hou J, Hong T, Ding Y, Nord N. Energy, economic, and environmental analysis of integration of thermal energy storage into district heating systems using waste heat from data centres. Energy 2021;219:119582. https://doi.org/10.1016/j.energy.2020.119582.

[31] TRNSYS. Transient system simulation tool. http://www.trnsys.com/;. [Accessed 8 April 2021].

[32] Hyrzyński R, Ziółkowski P, Gotzman S, Kraszewski B, Ochrymiuk T, Badur J. Comprehensive thermodynamic analysis of the CAES system coupled with the underground thermal energy storage taking into account global, central and local level of energy conversion. Renew Energy 2021;169:379–403. https://doi.org/10.1016/j.renene.2020.12.123.

[33] Karasu H, Dincer I. Life cycle assessment of integrated thermal energy storage systems in buildings: a case study in Canada. Energy Build 2020;217:109940. https://doi.org/10.1016/j.enbuild.2020.109940.

[34] DLSC. Drake landing solar community. 2021. https://dlsc.ca/. [Accessed 8 April 2021].

[35] Wong B, Mesquita L. Drake landing solar community: financial summary and lessons learned. In: Proceedings of the ISES Solar World Congress; 2019. p. 482–93. 2019 Nov 4-7; Santiago, Chile; 2019.

[36] McDowell TP, Thornton JW. Simulation and model calibration of a large-scale solar seasonal storage system. In: Proceedings of the 3rd National Conference of IBPSA-USA; 2008 Jul 30-Aug 1; Berkeley, USA; 2008. p. 174–81.

[37] National Development and Reform Commission. Supervision and examination method for pricing cost of urban district heating. https://www.ndrc.gov.cn/yjzxDownload/gg3czjzgrjghsfgl.pdf;. [Accessed 6 October 2021].

[38] Zhang L, Li Y, Zhang H, Xu X, Yang Z, Xu W. A review of the potential of district heating system in Northern China. Appl Therm Eng 2021;188:116605. https://doi.org/10.1016/j.applthermaleng.2021.116605.

[39] National Bureau of Statistics of China. National data. 2021. https://data.stats.gov.cn/. [Accessed 8 April 2021].

[40] Guo J, Huang Y, Wei C. North-South debate on district heating: evidence from a household survey. Energy Pol 2015;86:295–302. https://doi.org/10.1016/j.enpol.2015.07.017.

[41] Liu W, Lund H, Mathiesen BV, Zhang X. Potential of renewable energy systems in China. Appl Energy 2011;88(2):518–25. https://doi.org/10.1016/j.apenergy.2010.07.014.

[42] Weiss W, Spörk-Dür M. Solar heat worldwide. https://www.iea-shc.org/Data/Sites/1/publications/Solar-Heat-Worldwide-2020.pdf;. [Accessed 8 April 2021].

[43] Solargis. Solar resource maps of China. https://solargis.com/maps-and-gis-data/download/china;. [Accessed 8 April 2021].

[44] Meteotest. Meteonorm software. Worldwide irradiation data. 2021. https://meteonorm.com/;. [Accessed 8 April 2021].

[45] Sketchup Trimble. https://www.sketchup.com/;. [Accessed 8 April 2021].

[46] Ministry of Housing and Urban-Rural Development of the People's Republic of China. Design standard for energy efficiency of residential buildings in severe cold and cold zones (JGJ 26-2018). Beijing: China Architecture & Building Press; 2018.

[47] Ministry of Housing and Urban-Rural Development of the People's Republic of China. Design standard for energy efficiency of residential buildings in hot summer and cold winter zones (JGJ 134-2010). Beijing: China Architecture & Building Press; 2010.

[48] Lizana J, Ortiz C, Soltero VM, Chacartegui R. District heating systems based on low-carbon energy technologies in Mediterranean areas. Energy 2017;120:397–416. https://doi.org/10.1016/j.energy.2016.11.096.

[49] Ministry of Housing and Urban-Rural Development of the People's Republic of China. Technical standard for solar water heating system of civil buildings (GB 50364-2018). Beijing: China Architecture & Building Press; 2018.

[50] Renaldi R, Friedrich D. Techno-economic analysis of a solar district heating system with seasonal thermal storage in the UK. Appl Energy 2019;236:388–400. https://doi.org/10.1016/j.apenergy.2018.11.030.

[51] Flynn C, Sirén K. Influence of location and design on the performance of a solar district heating system equipped with borehole seasonal storage. Renew Energy 2015;81:377–88. https://doi.org/10.1016/j.renene.2015.03.036.

[52] Sibbitt B, McClenahan D, Djebbar R, Thornton J, Wong B, Carriere J, et al. The performance of a high solar fraction seasonal storage district heating system - five years of operation. Energy Proc 2012;30:856–65. https://doi.org/10.1016/j.egypro.2012.11.097.

[53] Mesquita L, McClenahan D, Thornton J, Carriere J, Wong B. Drake landing solar community: 10 years of operation. In: Proceedings of the ISES Solar World Congress 2017; 2017 Oct 29-Nov 2; Abu Dhabi, UAE; 2017. p. 333–44.

[54] Su C, Madani H, Palm B. Heating solutions for residential buildings in China: current status and future outlook. Energy Convers Manag 2018;177:493–510. https://doi.org/10.1016/j.enconman.2018.10.005.

[55] Mauthner F, Herkel S. Technology and Demonstrators. Technical report subtask C - Part C1. 2016. http://task3.iea-shc.org/data/sites/1/publications/IEA-SHC-Task52-STC1-Classification-and-benchmarking-Report-2016-03-31.pdf;. [Accessed 8 April 2021].

[56] OECD. Inflation (CPI). https://doi.org/10.1787/eee82e6e-en. [Accessed 8 April 2021].

[57] OECD. Exchange rates. https://doi.org/10.1787/037ed317-en. [Accessed 8 April 2021].

[58] Harbin Development and Reform Commission. Clean winter heating implementation plan in Harbin (2019-2021). 2019. http://www.harbin.gov.cn/art/2020/1/7/art_24978_863216.html;. [Accessed 8 April 2021].

[59] Xue G, Song J, Kong X, Pan Y, Qi C, Li H. Prediction of natural gas consumption for city-level DHS based on attention GRU: a case study for a northern Chinese city. IEEE Access 2019;7:130685–99. https://doi.org/10.1109/ACCESS.2019.2940210.

[60] Ascione F, Bianco N, De Stasio C, Mauro GM, Vanoli GP. 5.21 Energy management in hospitals. In: Dincer I, editor. Comprehensive energy systems. Oxford: Elsevier; 2018. p. 827–54.

[61] Catolico N, Ge S, McCartney JS. Numerical modeling of a soil-borehole thermal energy storage system. Vadose Zone J 2016;15(1). https://doi.org/10.2136/vzj2015.05.0078.

[62] Rad FM, Fung AS, Rosen MA. An integrated model for designing a solar community heating system with borehole thermal storage. Energy Sustain Dev 2017;36:6–15. https://doi.org/10.1016/j.esd.2016.10.003.

[63] Lyu C, Leong WH, Zheng M, Jiang P, Yu F, Liu Y. Dynamic simulation and operating characteristics of ground-coupled heat pump with solar seasonal heat storage system. Heat Tran Eng 2019;41(9–10):840–50. https://doi.org/10.1080/01457632.2019.1576423.

[64] Hesaraki A, Holmberg S, Haghighat F. Seasonal thermal energy storage with heat pumps and low temperatures in building projects—a comparative review. Renew Sustain Energy Rev 2015;43:1199–213. https://doi.org/10.1016/j.rser.2014.12.002.

[65] Pinel P, Cruickshank CA, Beausoleil-Morrison I, Wills A. A review of available methods for seasonal storage of solar thermal energy in residential applications. Renew Sustain Energy Rev 2011;15(7):3341–59. https://doi.org/10.1016/j.rser.2011.04.013.

[66] Rosato A, Ciervo A, Ciampi G, Scorpio M, Sibilio S. Impact of seasonal thermal energy storage design on the dynamic performance of a solar heating system serving a small-scale Italian district composed of residential and school buildings. J Energy Storage 2019;25:100889. https://doi.org/10.1016/j.est.2019.100889.

[67] Javadi H, Mousavi Ajarostaghi SS, Rosen MA, Pourfallah M. Performance of ground heat exchangers: a comprehensive review of recent advances. Energy 2019;178:207–33. https://doi.org/10.1016/j.energy.2019.04.094.

[68] Zhang C, Song W, Sun S, Peng D. Parameter estimation of in-situ thermal response test with unstable heat rate. Energy 2015;88:497–505. https://doi.org/10.1016/j.energy.2015.05.074.

[69] Metz B, Davidson O, Coninck Hd, Loos M, Meyer L. IPCC special report on carbon dioxide capture and storage. New York: Cambridge University Press; 2005.

[70] Ming Z, Shaojie O, Yingjie Z, Hui S. CCS technology development in China: status, problems and countermeasures—based on SWOT analysis. Renew Sustain Energy Rev 2014;39:604–16. https://doi.org/10.1016/j.rser.2014.07.037.

[71] National Bureau of Statistics of China. China national economic and social development statistics bulletin 2020. 2021. http://www.stats.gov.cn/tjsj/zxfb/202102/t20210227_1814154.html;. [Accessed 6 October 2021].

[72] China Electricity Council. Research on the development plan of the electric power industry during the ''14th Five-Year Plan. 2021. https://cec.org.cn/detail/index.html?3-297199. [Accessed 6 October 2021].

[73] Xu Y, Yang Z, Yuan J. The economics of renewable energy power in China. Clean Technol Environ Policy 2021;23(4):1341–51. https://doi.org/10.1007/s10098-021-02031-0.

[74] Yang T, Liu W, Kramer GJ. Integrated assessment on the implementation of sustainable heat technologies in the built environment in Harbin, China. Energy Convers Manag 2023;279:116764. https://doi.org/10.1016/j.enconman.2023.116764.

[75] Zhou K, Mao J, Li Y, Zhang H. Performance assessment and techno-economic optimization of ground source heat pump for residential heating and cooling: a case study of Nanjing, China. Sustain Energy Technol Assessments 2020;40:100782. https://doi.org/10.1016/j.seta.2020.100782.

[76] Xia ZH, Jia GS, Ma ZD, Wang JW, Zhang YP, Jin LW. Analysis of economy, thermal efficiency and environmental impact of geothermal heating system based on life cycle assessments. Appl Energy 2021;303:117671. https://doi.org/10.1016/j.apenergy.2021.117671.